

Randomized Control of Wireless Temporal Coherence via Reconfigurable Intelligent Surface

João Henrique Inacio de Souza, Victor Croisfelt, Fabio Saggese, Taufik Abrão, and Petar Popovski

Abstract—A reconfigurable intelligent surface (RIS) can shape the wireless propagation channel by inducing controlled phase shift variations to the impinging signals. Multiple works have considered the use of RIS by time-varying configurations of reflection coefficients. In this work we use the RIS to control the channel coherence time and introduce a generalized discrete-time-varying channel model for RIS-aided systems. We characterize the temporal variation of channel correlation by assuming that a configuration of RIS' elements changes at every time step. The analysis converges to a randomized framework to control the channel coherence time by setting the number of RIS' elements and their phase shifts. The main result is a framework for a flexible block-fading model, where the number of samples within a coherence block can be dynamically adapted.

Index Terms—Reconfigurable intelligent surface (RIS), temporal correlation, fading.

I. INTRODUCTION

A reconfigurable intelligent surface (RIS) consists of a massive number of passive reflecting elements able to alter the phase shifts and possibly the amplitude of impinging wireless signals [1], thereby exerting control over the wireless propagation. Some RIS instances can be seen as passive holographic multiple-input multiple-output (MIMO) surfaces. Numerous use cases have been proposed to show how such control can benefit the communication between a transmitter (Tx) and a receiver (Rx), where the prevailing focus is on improving the communication performance [1]. However, relatively few works explore how to use the RIS to induce changes that induce temporal diversity in the wireless channel and avoid prolonged unfavorable propagation to a given user.

To illustrate, consider the channel aging problem that occurs due to Rx mobility which makes the channel state information (CSI) acquired by the Tx unreliable over time. Works as [2]–[5] suggest the use of an RIS to deal with this problem by compensating for the Doppler effects of mobility. The focus of these works typically relies on optimizing the RIS' configurations of the elements aiming to minimize the channel aging effect. In [6], a continuous-time propagation model is given and is used to configure the RIS in such a way that the received power is maximized whereas the delay and Doppler spread are minimized. The authors in [7] study the spatial-temporal correlation implied by the RIS when it is embedded in an isotropic scattering environment. Nevertheless, these

prior works do not analyze how the temporal channel statistics, such as the coherence time, can be modeled as a function of the properties of the RIS' elements. In this paper, we focus on studying how the RIS can shape temporal channel statistics by relying on a discrete-time-varying channel model. A closely related work is [8] where the authors proposed an RIS phase hopping scheme with the purpose of transforming a slow-fading into a fast-fading channel. This was achieved by randomly varying the RIS' configurations, significantly improving the outage performance without the need for CSI at the RIS. Nevertheless, this paper focuses on how the random variation of phases impacts the outage performance, while here we analyze temporal channel correlation that stems from the properties of the RIS.

We propose a generalized discrete-time-varying channel model for RIS-aided communication systems, showing how the part of the propagation environment controlled by the RIS shapes the discrete temporal channel statistics. We characterize the temporal variation of channel correlation as the RIS' reflections configuration changes at every time index. This analysis reveals how one can control the coherence time of the channel by changing the number of RIS' reflecting elements and their phase shift configurations. Our findings corroborate the results from [8], and prove the possibility of using the RIS to generate a flexible block-fading model.

Notation. Boldface lowercase \mathbf{a} and uppercase \mathbf{A} letters represent vectors and matrices, respectively. Calligraphic letters \mathcal{A} represent finite sets. Operators: transpose by $\{\cdot\}^T$, complex conjugate by $\{\cdot\}^*$, and real part by $\Re\{\cdot\}$. Important functions are: $\lfloor \cdot \rfloor$ the floor function, $\delta[\cdot]$ the Kronecker's delta function, and $\text{sinc}(\theta) = \frac{\sin(\theta)}{\theta}$. The expected value operator is $\mathbb{E}\{\cdot\}$ and, unless otherwise stated, it is taken w.r.t. the variable k . The complex Gaussian distribution is denoted as $\mathcal{CN}(\mu, \sigma^2)$ with mean μ and variance σ^2 , whereas a uniform random distribution over the range $[a, b]$ is $\mathcal{U}(a, b)$.

II. SYSTEM MODEL

The communication setup consists of one single-antenna Tx, one single-antenna Rx, and one RIS with $N \in \mathbb{Z}_+$ passive reflecting elements, operating in narrowband communication channel and in free space. The wireless channel consists of two distinct radio paths from the Tx to the Rx, the direct path and the reflected path controlled by the RIS, see Fig. 1. The index of the complex samples in the discrete-time domain is denoted by $k \in \mathbb{Z}$.

Considering the downlink, let $h_D[k] \in \mathbb{C}$ denote the channel coefficient from the Tx to the Rx, $g_n[k] \in \mathbb{C}$ denote the

J. H. I. de Souza and T. Abrão are with the Department of Electrical Engineering, Universidade Estadual de Londrina, Londrina, Brazil; E-mail: joaohis@outlook.com and taufik@uel.br.

V. Croisfelt, F. Saggese, and P. Popovski are with the Department of Electronic Systems, Aalborg University, Aalborg, Denmark; E-mail: {vcr, fasa, petar}@es.aau.dk.

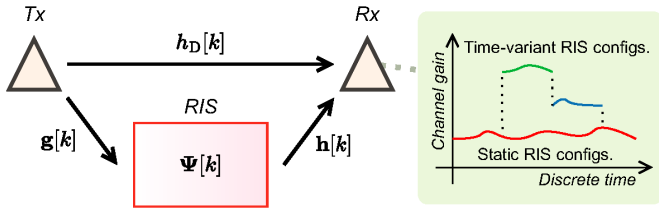


Figure 1. RIS-aided communication system, where the RIS' elements imposing time-variant reflection configurations can alter the channel response.

channel coefficient from the Tx to the n -th reflecting element of the RIS, and $h_n[k] \in \mathbb{C}$ denote the channel coefficient from the n -th reflecting element of the RIS to the Rx, $n \in \{1, \dots, N\}$. Let the channel vectors from the Tx to the RIS and from the RIS to the Rx be $\mathbf{g}[k] = [g_1[k], \dots, g_N[k]]^T$ and $\mathbf{h}[k] = [h_1[k], \dots, h_N[k]]^T$, respectively. Consider then that the n -th reflecting element of the RIS can induce a phase shift of $\phi_n[k] \in [0, 2\pi)$ upon the impinging signal with marginal impact on the signal's amplitude. Thus, we denote the RIS' configuration impressed at time k as the matrix $\Psi[k] = \text{diag}([\psi_1[k], \dots, \psi_N[k]]^T)$, whose n -th diagonal entry is the *reflection coefficient* $\psi_n[k] = e^{-j\phi_n[k]}$ of the n -th RIS element.¹ Using the narrowband model from [1], we assume that a RIS configuration is constant within the time of each sample k .² Moreover, we assume that the RIS' elements have a flat frequency response, preserving the coherence bandwidth of the equivalent channel, $B_c > 0$.³ The equivalent channel $h_{\text{eq}}[k] \in \mathbb{C}$ from the Tx to the Rx is then [1]:

$$\begin{aligned} h_{\text{eq}}[k] &= h_D[k] + \mathbf{g}^T[k] \Psi[k] \mathbf{h}[k], \\ &= \underbrace{h_D[k]}_{\text{Uncontrollable}} + \underbrace{\sum_{n=1}^N g_n[k] h_n[k] \psi_n[k]}_{\text{Controllable}}. \end{aligned} \quad (1)$$

Eq. (1) is made up of two different time-variant terms: the *uncontrollable component* depending only on the properties of the propagation environment, and the *controllable components* controlled by changing the RIS' configurations.

III. DISCRETE-TIME-VARYING CHANNEL MODEL

In this section, we present a discrete-time-varying model for the channels $h_D[k]$, $\mathbf{g}[k]$, and $\mathbf{h}[k]$ in order to understand the impact of switching the reflection coefficients of the RIS over the time index k . Based on such a model, we show how the temporal correlation of the equivalent channel behaves by characterizing its autocorrelation function (ACF) w.r.t. k .

¹The RIS is considered to have unitary attenuation to simplify the presentation. The generalization is considered to be straightforward.

²During the switching time from a configuration to another, the RIS can generate an unpredictable channel behavior. Throughout the paper, we assume that this effect is negligible considering that the switching time is much lower than the time reserved for each configuration.

³ B_c is inversely proportional to the *channel delay spread*, determined by the multiple reflection delays of the signal between the Tx and Rx.

A. The Model

Without loss of generality, let $h[k] \in \mathbb{C}$ denote a generic channel coefficient sample from one of the channels $h_D[k]$, $g_n[k]$, and $h_n[k]$. To represent both line-of-sight (LoS) and non-line-of-sight (NLoS) components, we assume the time-variant Rician fading model as follows [9]:

$$h[k] = \bar{h} + \check{h}[k], \quad (2)$$

where $\bar{h} \in \mathbb{C}$ denotes the time-invariant LoS channel component and $\check{h}[k] \in \mathbb{C}$ denotes the time-variant NLoS channel component. Specifically, the NLoS component is modeled as a stationary first-order autoregressive (AR(1)) random process with recurrence relation [10]–[12]⁴

$$\check{h}[k] = \alpha_h \check{h}[k-1] + \sqrt{1 - \alpha_h^2} \sigma_h w[k], \quad (3)$$

where $0 \leq \alpha_h < 1$ denotes the AR(1) parameter, $\sigma_h^2 > 0$ denotes the power of the NLoS component, and $w[k]$ is a white stationary complex Gaussian process such that $w[k] \sim \mathcal{CN}(0, 1)$. From (2) and the properties of the AR(1), it is straightforward to demonstrate that:

$$\mathbb{E}\{h[k]\} = \bar{h} \text{ and } \mathbb{E}\{|h[k]|^2\} = |\bar{h}|^2 + \sigma_h^2. \quad (4)$$

Hence, the Rice factor $\kappa_h > 0$ of $h[k]$ is defined as the ratio between the powers of the LoS and NLoS components,

$$\kappa_h = |\bar{h}|^2 / \sigma_h^2. \quad (5)$$

Given the channel model and the relationship between the powers of its time-invariant and -variant parts, we now define what are the intrinsic parameters to the environment, meaning that they are determined by the physical properties of the wireless propagation medium and the setup geometry, and *cannot* be directly controlled by the system designer.

Definition 1. (Set of Environmental Parameters) We denote as $\mathcal{E}_h = \{\alpha_h, \kappa_h, \sigma_h^2\}$ the set of environmental parameters.

B. Temporal Correlation of the Equivalent Channel

We now carry out an analysis of the correlation among the channel samples over the time index k . Our first result is summarized in the following lemma.

Lemma 1. Consider that the channel coefficients $h_D[k]$, $g_n[k]$, and $h_n[k]$, $\forall n$, follow the time-variant Rician model in eq. (2). Then, the ACF $R_{h_{\text{eq}}h_{\text{eq}}} : \mathbb{Z} \rightarrow \mathbb{R}$ of the equivalent channel is given by eq. (6) at the top of the next page, where $R_{\psi_n\psi_{n'}} : \mathbb{Z} \rightarrow \mathbb{R}$ is the cross-correlation function (CCF) of the RIS' reflection coefficients, calculated for the discrete-time delay τ as:

$$R_{\psi_n\psi_{n'}}[\tau] = \mathbb{E}\{\psi_n[k] \psi_{n'}^*[k - \tau]\}. \quad (7)$$

Proof. See Appendix A. \square

⁴In [10], the authors demonstrated that the AR model could be considered for the computer simulation of correlated fading channels, corroborating that low orders are appropriate for narrowband Doppler fading processes. Moreover, [11], [12] unveil that an AR(1) model is enough to capture most of the channel tap dynamics.

$$R_{h_{\text{eq}}h_{\text{eq}}}[\tau] = \mathbb{E} \{ h_{\text{eq}}[k] h_{\text{eq}}^*[k - \tau] \} = |\bar{h}_{\text{D}}|^2 + \alpha_{h_{\text{D}}}^{|\tau|} \sigma_{h_{\text{D}}}^2 + \sum_{n=1}^N \left(|\bar{g}_n|^2 + \alpha_{g_n}^{|\tau|} \sigma_{g_n}^2 \right) \left(|\bar{h}_n|^2 + \alpha_{h_n}^{|\tau|} \sigma_{h_n}^2 \right) R_{\psi_n \psi_n}[\tau] + \quad (6)$$

$$+ \sum_{n=1}^N \sum_{\substack{n'=1 \\ n' \neq n}}^N \bar{g}_n \bar{g}_{n'}^* \bar{h}_n \bar{h}_{n'}^* R_{\psi_n \psi_{n'}}[\tau] + 2\Re \left\{ \bar{h}_{\text{D}}^* \sum_{n=1}^N \bar{g}_n \bar{h}_n \mathbb{E} \{ \psi_n[k] \} \right\}.$$

From the above result, one can note that the channel ACF inherits the *uncontrollable* part and the *controllable* part from the equivalent channel in eq. (1).

IV. A RANDOMIZED FRAMEWORK FOR CONTROLLING THE TEMPORAL CORRELATION

We start by providing a general framework that describes how to control the temporal correlation by using Lemma 1 to set the number of RIS' reflecting elements N and/or designing their configuration $\{\psi_n[k]\}_{n=1}^N$. Note that through N we select an RIS of sufficient size to meet the system's temporal correlation requirements. Then, we study the case with uniformly distributed phase shifts, as in [8].

A. Temporal Correlation under Random Phase Shifts

We first make the following simplifying assumptions. **(1)** There is no direct path from the Tx to the Rx, *i.e.*, $h_{\text{D}}[k] = 0$. This holds when obstacles block the direct path between the Tx and the Rx, as in dense urban scenarios and industries. **(2)** The LoS components are predominant in the channels from the Tx to the RIS, *i.e.*, $\kappa_{g_n} \rightarrow \infty$ dB, $\forall n$. Therefore, these channels are static, *i.e.*, $g_n[k] = \bar{g}_n, \forall n$. This can be justified by the fact that the Tx and the RIS do not move and the deployment of the RIS is chosen so as to enhance the LoS components between the Tx and the RIS. Using these assumptions, the equivalent channel in (1) can be rewritten as:

$$h'_{\text{eq}}[k] = \bar{\mathbf{g}}^T \Psi[k] \mathbf{h}[k], \quad (8)$$

and its ACF is given by:

$$R_{h'_{\text{eq}}h'_{\text{eq}}}[\tau] = \sum_{n=1}^N |\bar{g}_n|^2 \left(|\bar{h}_n|^2 + \alpha_{h_n}^{|\tau|} \sigma_{h_n}^2 \right) R_{\psi_n \psi_n}[\tau] + \sum_{n=1}^N \sum_{\substack{n'=1 \\ n' \neq n}}^N \bar{g}_n \bar{g}_{n'}^* \bar{h}_n \bar{h}_{n'}^* R_{\psi_n \psi_{n'}}[\tau], \quad (9)$$

where $\bar{\mathbf{g}} = [\bar{g}_1, \dots, \bar{g}_N]^T$ and $\bar{\mathbf{h}} = [\bar{h}_1, \dots, \bar{h}_N]^T$. We further assume that the N channels from the RIS' elements to the Rx share the same set of environmental parameters $\mathcal{E} = \{\alpha, \kappa, \sigma^2\}$, where $\alpha_{h_n} = \alpha$, $\kappa_{h_n} = \kappa$, and $\sigma_{h_n}^2 = \sigma^2, \forall n$. This assumption is valid when considering that the process which introduces the time variations is the same for all N channels and that the receptions occur in the far-field regime [10]. Now, let us assume that the phase shifts at a given time k are drawn from a uniform random distribution:

$$\phi'_n[k] \sim \mathcal{U}(\pi - \theta, \pi + \theta), \quad \forall n, \quad (10)$$

where $\theta \in [0, \pi]$ is the phase shifts distribution parameter. Then, the CCF of the RIS' reflection coefficients is:

$$R_{\psi'_n \psi'_{n'}}[\tau] = \begin{cases} 1, & \text{if } n = n' \\ \text{sinc}^2(\theta), & \text{otherwise} \end{cases}, \quad (11)$$

where we used eq. (7). Substituting (11) into eq. (9) and considering that $|\bar{\mathbf{g}}^T \bar{\mathbf{h}}|^2 = \sum_{n=1}^N \sum_{n'=1}^N \bar{g}_n \bar{g}_{n'}^* \bar{h}_n \bar{h}_{n'}^*$ results in the ACF of the equivalent channel in eq. (12) at the bottom of the page, with

$$\eta = \left| \frac{\bar{\mathbf{g}}^T \bar{\mathbf{h}}}{\|\bar{\mathbf{g}}\|_2 \|\bar{\mathbf{h}}\|_2} \right|^2. \quad (13)$$

Specifically, the equality (a) in eq. (12) results from the Rice factor in eq. (5), *i.e.*, from substituting the term $\|\bar{\mathbf{h}}\|_2^2 = \sum_{n=1}^N |\bar{h}_n|^2$ by $N\kappa\sigma^2$. Also, from the triangle inequality, η lies between $[0, 1]$ and is a measure of *orthogonality* between the LoS components of the channels $\mathbf{g}[k]$ and $\mathbf{h}[k]$, depending on N and the positions of the RIS, Tx, and Rx [13].

By using the results for the CCF and ACF, we derive the correlation coefficient between two channel samples delayed by $|\tau|$ samples, as shown in eq. (14) at the bottom of the page. One can notice that the temporal channel correlation depends on: *i)* the delay $|\tau|$ between the channel samples in discrete time, *ii)* the environmental parameters set \mathcal{E} , *iii)* the number of RIS' reflecting elements N , and *iv)* the parameter

$$R_{h'_{\text{eq}}h'_{\text{eq}}}[\tau] = (1 - \text{sinc}^2(\theta)) \left(\sum_{n=1}^N |g_n|^2 |\bar{h}_n|^2 + \sigma^2 \|\bar{\mathbf{g}}\|_2^2 \right) \delta[\tau] + \text{sinc}^2(\theta) \left(|\bar{\mathbf{g}}^T \bar{\mathbf{h}}|^2 + \alpha^{|\tau|} \sigma \|\bar{\mathbf{g}}\|_2^2 \right),$$

$$\stackrel{(a)}{=} \sigma^2 \|\bar{\mathbf{g}}\|_2^2 \left[(1 - \text{sinc}^2(\theta)) (\kappa + 1) \delta[\tau] + \text{sinc}^2(\theta) (N\kappa\eta + \alpha^{|\tau|}) \right]. \quad (12)$$

$$\rho[\tau] = \frac{R_{h'_{\text{eq}}h'_{\text{eq}}}[\tau]}{R_{h'_{\text{eq}}h'_{\text{eq}}}[0]} = \frac{(1 - \text{sinc}^2(\theta)) (\kappa + 1) \delta[\tau] + \text{sinc}^2(\theta) (N\kappa\eta + \alpha^{|\tau|})}{(1 - \text{sinc}^2(\theta)) (\kappa + 1) + \text{sinc}^2(\theta) (N\kappa\eta + 1)}. \quad (14)$$

that determines the range of the phase shifts' distribution θ . We make the following remarks about the obtained result.

Remark 1. Regarding κ and η , it is worth noting that, in the absence of a LoS path component from the RIS to the receiver, *i.e.*, $\kappa \rightarrow -\infty$ dB, or when the LoS components are perfectly orthogonal, *i.e.*, $\eta = 0$, the channel correlation is determined only by α and θ . On the other hand, if $\kappa > 0$ and $\eta > 0$, the correlation coefficient can also be altered by setting N .

Remark 2. Regarding the distribution parameter θ , we analyze how the temporal channel correlation behaves in the extreme values of its range, $[0, \pi]$. When $\theta = 0$, the resulting *correlation coefficient* from (14) simplifies to:

$$\rho[\tau]|_{\theta=0} = \frac{N\kappa\eta + \alpha^{|\tau|}}{N\kappa\eta + 1}. \quad (15)$$

In this case, note that one can control the temporal correlation *only* by selecting the number of RIS' elements N . On the other hand, when $\theta = \pi$, the correlation coefficient becomes:

$$\rho[\tau]|_{\theta=\pi} = \delta[\tau]. \quad (16)$$

Now, observe that the channel samples are totally uncorrelated, corroborating with the findings of [8]. Recall that the authors of [8] used $\phi'_n[k] \sim \mathcal{U}(0, 2\pi)$ to transform a slow-fading channel into a fast-fading one, improving reliability-related metrics. Hence, by tuning θ and given N , we can control the temporal correlation to values in the interval $[\rho[\tau]|_{\theta=\pi}, \rho[\tau]|_{\theta=0}]$.

B. Controlling the Temporal Correlation

Based on Remark 2, we present a method to design the phase shifts distribution parameter θ to obtain the desired channel correlation between samples separated from each other by a desired delay. This is based on the following:

Definition 2. (Project Requirements) The tuple of *project requirements* is $p = (\tilde{\rho}, \tilde{\tau})$, where $0 \leq \tilde{\rho} \leq 1$ is the desired correlation coefficient of two-channel samples delayed by $\tilde{\tau} \in \mathbb{Z}_+$ samples.

Method. From eq. (14) and for a constant N , the value of θ for obtaining a channel correlation coefficient $\rho[\pm\tilde{\tau}] = \tilde{\rho}$ is:

$$\theta = \underline{\theta}(p) = \text{sinc}^{-1} \left(\sqrt{\frac{(\kappa + 1)\tilde{\rho}}{\tilde{\rho}\kappa + (1 - \tilde{\rho})N\kappa\eta + \alpha^{|\tilde{\tau}|}}} \right), \quad (17)$$

where $\text{sinc}^{-1}(\cdot)$ is the inverse function of $\text{sinc}(\cdot)$ with codomain over the interval $[0, \pi]$.⁵ By taking into account that $\theta \in [0, \pi]$, the argument in the right-hand side (RHS) of (17) must lie in the interval $[0, 1]$. Given this, we define the set of feasible project requirements as:

$$\mathcal{P}_{\text{feas.}}^{(\theta)} = \left\{ (\tilde{\rho}, \tilde{\tau}) \in \mathbb{R}_+ \times \mathbb{Z}_+ \mid 0 \leq \tilde{\rho} \leq \frac{N\kappa\eta + \alpha^{|\tilde{\tau}|}}{N\kappa\eta + 1} \right\}. \quad (18)$$

⁵In the domain $[0, \pi]$, the $\text{sinc}(\cdot)$ function is partially invertible since it becomes bijective. In the absence of a closed-form expression for $\text{sinc}^{-1}(\cdot)$, numerical methods can be used to calculate it with the required precision.

From the above, one can note that the feasible channel correlation is upper-bounded by the environmental parameters \mathcal{E} and the number of RIS reflecting elements N .

Remark 3. In Remark 1, we have observed that one can also control the correlation coefficient by changing N . We now give an additional result showing the achievable channel correlation when opting for designing N . We assume that the RIS, Tx, and Rx are positioned in a way that η does not vary with N .⁶ Considering a constant θ , the value of N for obtaining a correlation coefficient $\rho[\pm\tilde{\tau}] = \tilde{\rho}$ is:

$$\underline{N}(p) = \left\lfloor \frac{(1 - \text{sinc}^2(\theta))(\kappa + 1) + \text{sinc}^2(\theta)(\tilde{\rho} - \alpha^{|\tilde{\tau}|})}{\text{sinc}^2(\theta)(1 - \tilde{\rho})\kappa\eta} \right\rfloor, \quad (19)$$

with $N = \underline{N}(p)$. Knowing that $N \geq 1$ and that the denominator of the argument at the RHS of (19) must be nonzero, the set of feasible project requirements can be derived as:

$$\mathcal{P}_{\text{feas.}}^{(N)} = \{ (\tilde{\rho}, \tilde{\tau}) \in \mathbb{R}_+ \times \mathbb{Z}_+ \mid \tilde{\rho}_{\min} \leq \tilde{\rho} < 1 \}, \text{ where} \quad (20)$$

$$\tilde{\rho}_{\min} = \frac{\text{sinc}^2(\theta)(\kappa\eta + \alpha^{|\tilde{\tau}|}) - (1 - \text{sinc}^2(\theta))(\kappa + 1)}{\text{sinc}^2(\theta)(\kappa\eta + 1)}. \quad (21)$$

From this, one can note that the achievable channel correlation by setting the number of RIS' elements N is lower-bounded by the environmental parameters \mathcal{E} and the parameter θ .

To get an overview of the condition in which Remark 3 is valid, Fig. 2 depicts how η changes with N considering different Rx positions. The LoS channel vectors are calculated with the model in [13]. Considering the *right-handed Cartesian* coordinates system, the RIS is placed parallel to the xy -plane with center at coordinates $(0, 0, 5)$, while the Tx is at coordinates $(-10, 0, 0)$. When the Rx position is symmetric to the Tx one w.r.t. the RIS center, $\eta = 1$ is constant. So Remark 3 is valid for position $(10, 0, 0)$. In position $(15, 0, 0)$, it may be valid for $N < 100$ due to the low variation of η in this region. However, it does not apply for positions $(10, 2, 0)$ and $(10, 10, 0)$ due to the high-amplitude oscillations of η with N .

V. SIMULATION RESULTS

In this section, we exemplify by numerical results how the method proposed in Subsection IV-B can be applied to obtain a given project requirement $p = (\tilde{\rho}, \tilde{\tau})$. The results and their respective simulation parameters are given in Figs. 3 and 4. In the simulations, the coordinate system, the RIS and

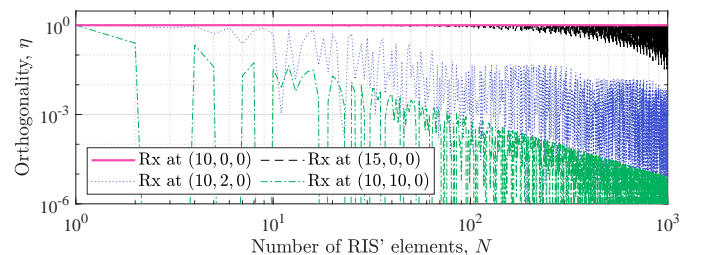
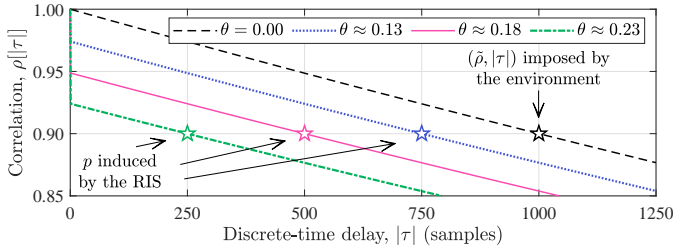
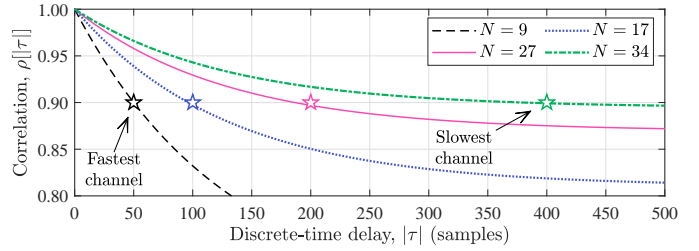


Figure 2. Orthogonality between the LoS components as a function of N .

⁶We leave the analysis of the case where η varies with N for future works.



(a) $\alpha = 1 - 1.12 \times 10^{-4}$, $\kappa = 6$ dB $N = 100$, Rx at (10, 10, 0)



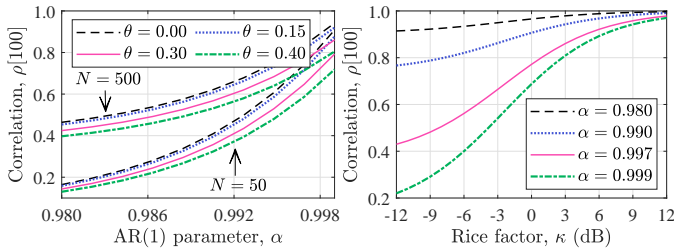
(b) $\alpha = 0.992$, $\kappa = -6$ dB, $\theta = 0$, Rx at (15, 0, 0)

Figure 3. Channel temporal correlation. The markers indicate the points where the correlation should reach 0.9 according to the project requirements p .

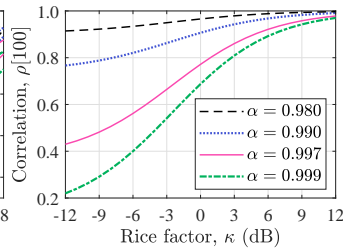
Tx positions, and the method to compute the LoS channel components are the same as in Fig. 2.

Fig. 3a depicts the correlation achieved by different θ with a fixed $N = 100$. From (10), recall that $\theta = 0$ implies static RIS phase shifts equal to π . Under this condition, α in this result is calculated by eq. (15) to obtain $\rho[1000]_{\theta=0} = 0.9$. For the cases where $\theta > 0$, the phase shifts distribution parameter θ is calculated by eq. (17) to obtain a correlation of $\tilde{\rho} = 0.9$ at the time delays $\tilde{\tau} \in \{250, 500, 750\}$. This result shows that the proposed method can change the temporal channel statistics imposed by the environment. In the sequel, Fig. 3b depicts the correlation obtained by different N . In this result, α is calculated using the aforementioned method, but now to obtain $\rho[50]_{\theta=0, N=9} = 0.9$. The values for $N > 9$ are calculated by eq. (19) to yield a correlation of $\tilde{\rho} = 0.9$ at the time delays $\tilde{\tau} \in \{100, 200, 400\}$. Such a result reveals that a fast channel, *i.e.*, a channel with a fast decay correlation, can be slowed down by increasing the number of elements of the RIS.

Fig. 4a shows the impact of θ and N in modifying the correlation at $|\tau| = 100$ as a function of α , representing different environmental conditions. It demonstrates that the correlation changes quickly with little change in α , justifying the use of the AR(1) model to represent both slow- and fast-fading channels. Then, Fig. 4b depicts the correlation at $|\tau| = 100$ as a function of κ and under different α . This result reveals that high κ yields correlation values close to 1 due to the significant increase on the power of the deterministic part of the channel $\bar{\mathbf{h}}$ relatively to the stochastic one $\{\tilde{h}_n\}_{n=1}^N$. In other words, as expected, the higher the κ parameter, the lower the impact of the RIS in controlling the environment. It is worth mentioning that low κ is typical in scenarios with partially blocked LoS and/or environments with rich scattering.



(a) $\kappa = 6$ dB, Rx at (10, 10, 0)



(b) $N = 100$, $\theta = 0$, Rx at (10, 2, 0)

Figure 4. Channel temporal correlation as a function of (a) α and (b) κ .

VI. TOWARDS A FLEXIBLE BLOCK-FADING MODEL

In this section, we extend the classical block-fading model [14], [15] to account for the channel correlation control based on the randomized framework proposed in Section IV. Define a *coherence block* as a resource block consisting of a number of subcarriers and time samples where the equivalent channel response z can be approximated as constant and flat-fading. Specifically, each coherence block has $\Delta_c = B_c T_c$ complex-valued samples, where $T_c > 0$ is the channel coherence time. Moreover, the channel response (power gain) z of this discrete-time channel follows a given distribution $z \sim f_Z$. For example, for Rayleigh fading channels, f_Z is exponential. The RIS-enabled control discussed in Section IV can be used to create coherent blocks with different lengths, where the coherence time relates to the discrete-time interval $\tilde{\tau}$. Recall that the channel coherence time is defined as the range of time span values over which the channel ACF is approximately nonzero [15]. Therefore, using the RIS to shape the ACF of the equivalent channel is a path to control T_c and, consequently, changing Δ_c . This generation of coherence blocks with a flexible number of samples can be done by setting θ and N to obtain a project requirement p as described respectively by eqs. (17) and (19). Particularly, this flexible block-fading model can improve how the resources are leveraged, enabling the on-demand creation of blocks according to the availability of services with different performance requirements over time.

VII. CONCLUSION

In this paper, we have studied how an RIS can change the temporal statistics of the wireless propagation channel by analyzing the correlation among channel samples using the introduced discrete-time-varying channel model. Then, we proposed a randomized framework to control the relative channel coherence time by setting the number of RIS' elements and designing the distribution of their reflection coefficients, whose effectiveness is corroborated by simulation results. Our results demonstrate the possibility of redefining the resource allocation problem as we know it today by creating a flexible block-fading model based on the proposed framework.

APPENDIX A

PROOF OF THE ACF OF THE EQUIVALENT CHANNEL

Recalling that $h_D[k]$, $\mathbf{g}[k]$, $\mathbf{h}[k]$, and $\Psi[k]$ are mutually independent, the ACF of eq. (1) is given by the sum:

$$R_{h_{\text{eq}}h_{\text{eq}}}[\tau] = \mathbb{E} \{ h_{\text{eq}}[k] h_{\text{eq}}^*[k - \tau] \} = S_1 + S_2 + S_3, \quad (22)$$

$$\text{where } S_1 = \mathbb{E} \{ h_D[k] h_D^*[k - \tau] \}, \quad (23)$$

$$S_2 = \mathbb{E} \left\{ \left(\mathbf{g}^T[k] \Psi[k] \mathbf{h}[k] \right) \times \left(\mathbf{g}^T[k - \tau] \Psi[k - \tau] \mathbf{h}[k - \tau] \right)^* \right\}, \text{ and} \quad (24)$$

$$S_3 = \mathbb{E} \left\{ h_D[k] \left(\mathbf{g}^T[k - \tau] \Psi[k - \tau] \mathbf{h}[k - \tau] \right)^* \right\} + \mathbb{E} \left\{ h_D^*[k - \tau] \left(\mathbf{g}^T[k] \Psi[k] \mathbf{h}[k] \right) \right\}. \quad (25)$$

Now we evaluate each term independently. Initially, due to the model in (2) adopted for $h_D[k]$, S_1 can be rewritten as:

$$\begin{aligned} S_1 &= \mathbb{E} \left\{ \left(\bar{h}_D + \check{h}_D[k] \right) \left(\bar{h}_D + \check{h}_D[k - \tau] \right)^* \right\} \\ &= |\bar{h}_D|^2 + \mathbb{E} \{ \check{h}_D[k] \check{h}_D^*[k - \tau] \} + \\ &\quad + \mathbb{E} \{ \bar{h}_D \check{h}_D^*[k - \tau] \} + \mathbb{E} \{ \check{h}_D^* \bar{h}_D[k] \}. \end{aligned} \quad (26)$$

Since \bar{h}_D is deterministic and $\check{h}_D[k]$ is an AR(1) random process as per (3), the expectations are given respectively by:

$$\begin{cases} \mathbb{E} \{ \check{h}_D[k] \check{h}_D^*[k - \tau] \} = \alpha_{\check{h}_D}^{|\tau|} \sigma_{\check{h}_D}^2, \\ \mathbb{E} \{ \bar{h}_D \check{h}_D^*[k - \tau] \} = \mathbb{E} \{ \check{h}_D^* \bar{h}_D[k] \} = 0. \end{cases} \quad (27)$$

So, S_1 can be rewritten as:

$$S_1 = |\bar{h}_D|^2 + \alpha_{\check{h}_D}^{|\tau|} \sigma_{\check{h}_D}^2. \quad (28)$$

Expanding the multiplications in S_2 results in

$$S_2 = \sum_{n=1}^N \sum_{n'=1}^N P_1 P_2 P_3, \quad (29)$$

$$\text{where } \begin{cases} P_1 = \mathbb{E} \{ g_n[k] g_{n'}[k - \tau] \}, \\ P_2 = \mathbb{E} \{ h_n[k] h_{n'}[k - \tau] \}, \\ P_3 = \mathbb{E} \{ \psi_n[k] \psi_{n'}[k - \tau] \} = R_{\psi_n \psi_{n'}}[\tau], \end{cases} \quad (30)$$

with $R_{\psi_n \psi_{n'}}$ defined in eq. (7). From the model in eq. (2) adopted for $\mathbf{g}[k]$ and $\mathbf{h}[k]$, and recalling that $\{g_n[k]\}_{n=1}^N$ and $\{h_n[k]\}_{n=1}^N$ are mutually independent, P_1 and P_2 result

$$P_1 = \begin{cases} |\bar{g}_n|^2 + \alpha_{g_n}^{|\tau|} \sigma_{g_n}^2, & \text{if } n = n' \\ \bar{g}_n \bar{g}_{n'}^*, & \text{otherwise} \end{cases}, \quad (31)$$

$$P_2 = \begin{cases} |\bar{h}_n|^2 + \alpha_{h_n}^{|\tau|} \sigma_{h_n}^2, & \text{if } n = n' \\ \bar{h}_n \bar{h}_{n'}^*, & \text{otherwise} \end{cases}. \quad (32)$$

While the results for $n = n'$ are based on the derivation of S_1 , the results for $n \neq n'$ come from the mean of the time-variant channel coefficient in eq. (4). Therefore, given the results for P_1 , P_2 , and P_3 , we can rewrite S_2 as:

$$\begin{aligned} S_2 &= \sum_{n=1}^N \sum_{n'=1, n' \neq n}^N \bar{g}_n \bar{g}_{n'}^* \bar{h}_n \bar{h}_{n'}^* R_{\psi_n \psi_{n'}}[\tau] + \\ &\quad + \sum_{n=1}^N \left(|\bar{g}_n|^2 + \alpha_{g_n}^{|\tau|} \sigma_{g_n}^2 \right) \left(|\bar{h}_n|^2 + \alpha_{h_n}^{|\tau|} \sigma_{h_n}^2 \right) R_{\psi_n \psi_n}[\tau]. \end{aligned} \quad (33)$$

In S_3 , the expectation of each multiplication can be rewritten as the multiplication of the expected value of each term:

$$S_3 = \bar{h}_D \bar{\mathbf{g}}^H \mathbb{E} \{ \Psi^*[k - \tau] \} \bar{\mathbf{h}}^* + \bar{h}_D^* \bar{\mathbf{g}}^T \mathbb{E} \{ \Psi[k] \} \bar{\mathbf{h}}. \quad (34)$$

Expanding the results of the multiplications in the summations:

$$S_3 = \bar{h}_D \sum_{n=1}^N \bar{g}_n^* \bar{h}_n^* \mathbb{E} \{ \psi_n^*[k - \tau] \} + \bar{h}_D^* \sum_{n=1}^N \bar{g}_n \bar{h}_n \mathbb{E} \{ \psi_n[k] \}. \quad (35)$$

Considering that $\{\psi_n[k]\}_{n=1}^N$ are wide-sense stationary (WSS) random processes, S_3 can be rewritten as:

$$S_3 = 2\Re \left\{ \bar{h}_D^* \sum_{n=1}^N \bar{g}_n \bar{h}_n \mathbb{E} \{ \psi_n[k] \} \right\}. \quad (36)$$

Finally, substituting eqs. (28), (33), and (36) into eq. (22), we obtain eq. (6), completing the proof. \square

REFERENCES

- [1] E. Björnson, H. Wymeersch, B. Matthiesen, P. Popovski, L. Sanguinetti, and E. de Carvalho, "Reconfigurable intelligent surfaces: A signal processing perspective with wireless applications," *IEEE Signal Processing Magazine*, vol. 39, no. 2, pp. 135–158, Feb. 2022.
- [2] Y. Chen, Y. Wang, and L. Jiao, "Robust transmission for reconfigurable intelligent surface aided millimeter wave vehicular communications with statistical CSI," *IEEE Transactions on Wireless Communications*, vol. 21, no. 2, pp. 928–944, Feb. 2022.
- [3] Y. Zhang, J. Zhang, H. Xiao, D. W. K. Ng, and B. Ai, "Channel aging-aware precoding for RIS-aided multi-user communications," *IEEE Transactions on Vehicular Technology*, pp. 1–13, Sept. 2022, early access.
- [4] W. Jiang and H. D. Schotten, "Performance impact of channel aging and phase noise on intelligent reflecting surface," *IEEE Communications Letters*, vol. 27, no. 1, pp. 347–351, Jan. 2023.
- [5] A. Papazafeiropoulos, I. Krikidis, and P. Kourtessis, "Impact of channel aging on reconfigurable intelligent surface aided massive MIMO systems with statistical CSI," *IEEE Transactions on Vehicular Technology*, vol. 72, no. 1, pp. 689–703, Jan 2023.
- [6] B. Matthiesen, E. Björnson, E. De Carvalho, and P. Popovski, "Intelligent reflecting surface operation under predictable receiver mobility: A continuous time propagation model," *IEEE Wireless Communications Letters*, vol. 10, no. 2, pp. 216–220, Feb. 2021.
- [7] S. Sun and H. Yan, "Small-scale spatial-temporal correlation and degrees of freedom for reconfigurable intelligent surfaces," *IEEE Wireless Communications Letters*, vol. 10, no. 12, pp. 2698–2702, Dec. 2021.
- [8] K.-L. Besser and E. A. Jorswieck, "Reconfigurable intelligent surface phase hopping for ultra-reliable communications," *IEEE Transactions on Wireless Communications*, vol. 21, no. 11, pp. 9082–9095, Nov. 2022.
- [9] A. Kurt, M. B. Salman, U. B. Sarac, and G. M. Guvensen, "An adaptive-iterative nonlinear interference cancellation in time-varying full-duplex channels," *IEEE Transactions on Vehicular Technology*, pp. 1–16, Sept. 2022, early access.
- [10] K. Baddour and N. Beaulieu, "Autoregressive modeling for fading channel simulation," *IEEE Transactions on Wireless Communications*, vol. 4, no. 4, pp. 1650–1662, July 2005.
- [11] K. T. Truong and R. W. Heath, "Effects of channel aging in massive MIMO systems," *Journal of Communications and Networks*, vol. 15, no. 4, pp. 338–351, Aug. 2013.
- [12] H. S. Wang and P.-C. Chang, "On verifying the first-order Markovian assumption for a Rayleigh fading channel model," *IEEE Transactions on Vehicular Technology*, vol. 45, no. 2, pp. 353–357, May 1996.
- [13] A. Albanese, F. Devoti, V. Sciancalepore, M. Di Renzo, and X. Costa-Pérez, "MARISA: A self-configuring metasurfaces absorption and reflection solution towards 6G," in *IEEE INFOCOM 2022 - IEEE Conference on Computer Communications*, 2-5 May 2022, pp. 250–259.
- [14] E. Björnson, J. Hoydis, and L. Sanguinetti, "Massive MIMO networks: Spectral, energy, and hardware efficiency," *Foundations and Trends® in Signal Processing*, vol. 11, no. 3-4, pp. 154–655, 2017.
- [15] A. Goldsmith, *Wireless Communications*. USA: Cambridge University Press, 2005.